Comparison of the $^{13}C+^{16}O$ reaction with $^{12}C+^{17}O$

R. M. Freeman, F. Haas, A. Morsad, and C. Beck
Centre de Recherches Nucléaires and Université Louis Pasteur, 67037 Strasbourg CEDEX, France
(Received 12 October 1988)

The $^{13}C+^{16}O$ reaction has been studied by the kinematic coincidence technique in the $E_{c.m.}$ range between 19 and 30 MeV. Angular distributions and excitation functions were compared with results from $^{12}C+^{17}O$ over the same energy range. Notable differences were found between the elastic angular distributions for the two reactions. Optical-model fits were performed to determine which parameters were sensitive to these differences. Broad structures, like shape resonances, were most apparent in the $^{13}C+^{16}O$ reaction, particularly for the excitation of collective states. Transfer reactions involving single-particle states show a more complex energy dependence.

I. INTRODUCTION

The study of the $^{12}C+^{17}O$ reaction which we recently published[1,2] was motivated by the possibility that the Landau-Zener promotion mechanism may strongly influence the inelastic scattering to the first excited state of ^{17}O. In this respect the $^{13}C+^{16}O$ entrance channel is different as there is no simple path by which a nucleon can be promoted to another orbital. A comparison between the two reactions was therefore desirable. However, only sparse experimental results in the appropriate bombarding energy range were available. Some measurements were reported by Westfall and Zaidi[3] for 36 MeV ^{13}C on ^{16}O, and Parks *et al.*[4] have measured excitation functions for the elastic channel at some angles. We have consequently supplemented our $^{12}C+^{17}O$ results with similar measurements on the $^{13}C+^{16}O$ system over an equivalent energy range.

The differences between the two entrance channels $^{13}C+^{16}O$ and $^{12}C+^{17}O$ appear to be rather small at first sight. The valence neutron is weakly bound (4.95 MeV) to a ^{12}C core in one system and in the other it is even more weakly bound (4.14 MeV) to ^{16}O. However, the collision dynamics will depend on a number of single-particle and collective variables which change from one system to the other. On one hand there is the spherical nucleus ^{16}O as opposed to the deformed nucleus ^{12}C, and on the other hand the valence neutron occupies a $p_{1/2}$ orbital in ^{13}C whereas it occupies a $d_{5/2}$ orbital in ^{17}O.

Though the results for the $^{13}C+^{16}O$ reaction will be the subject of this article, we will also include a certain number of results for the $^{12}C+^{17}O$ reaction for comparison.

II. EXPERIMENT

The $^{13}C+^{16}O$ reaction was studied using the same detection system set up as for one of the $^{12}C+^{17}O$ experiments.[1] Beams of ^{16}O from the Strasbourg MP tandem Van de Graaff bombarded a ^{13}C target nominally 22 $\mu m/cm^2$ thick. The incident beam energies were chosen to correspond to the same center-of-mass energies of our $^{12}C+^{17}O$ run where the ^{17}O energies ranged from 46 to 70 MeV in steps of 2 MeV.

There were two features of the data analysis which merit comment. Firstly, the ^{13}C target contained a significant ^{12}C contaminant. It was thus essential in this case to impose more selective conditions during the data analysis. Secondly, the $^{13}C+^{16}O$ cross sections were normalized to the $^{12}C+^{17}O$ data by applying the principle of detailed balance to the common channel $^{12}C_{g.s.}+^{17}O_{g.s.} \rightleftarrows ^{13}C_{g.s.}+^{16}O_{g.s.}$. This was facilitated because the measurements were taken in steps of $E_{c.m.}=0.83$ MeV, which is close to 0.80 MeV, the difference in binding energy between the two systems. Thus, the reverse reactions could be directly compared at approximately the same energy in the compound system (the slight energy discrepancy is smaller than the energy loss in the target). The cross-section ratios between the reverse reactions were determined at each energy and found to be generally within $\pm 5\%$ of an average value. As there was little evidence for any change in the ^{13}C target thickness during the experiment, this average value was used for the definitive normalizations.

Q-value spectra of all the four possible combinations of $^{13}C+^{16}O$ and $^{12}C+^{17}O$ as entrance and exit channels are shown in Fig. 1. These spectra result from angular cuts through the experimental data taken in roughly equivalent conditions. The angular distributions were determined from similar spectra where the angular slices were thinner. After applying geometrical and center-of-mass corrections, the intensities were normalized to construct the angular distributions like the examples displayed in Fig. 2. The $^{13}C+^{16}O$ angular distributions are compared in this figure with the $^{12}C+^{17}O$ data for the same energy in the compound system and the same four outgoing channels. The common channel $^{13}C+^{16}O \rightleftarrows ^{12}C+^{17}O$ shows an identical angular distribution, irrespective of direction, as expected for a reversible process, but their cross sections are different principally due to a factor of 3.0, the statistical spin term.

The energy resolution did not permit other channels to be easily extracted from the data. The strong peaks in the $^{13}C+^{16}O$ inelastic channels, for example, correspond to the (6.06-6.13) MeV doublet of ^{16}O and the (3.68-3.85) MeV doublet of ^{13}C. At one energy we verified that the cross sections for these two doublets showed no strong

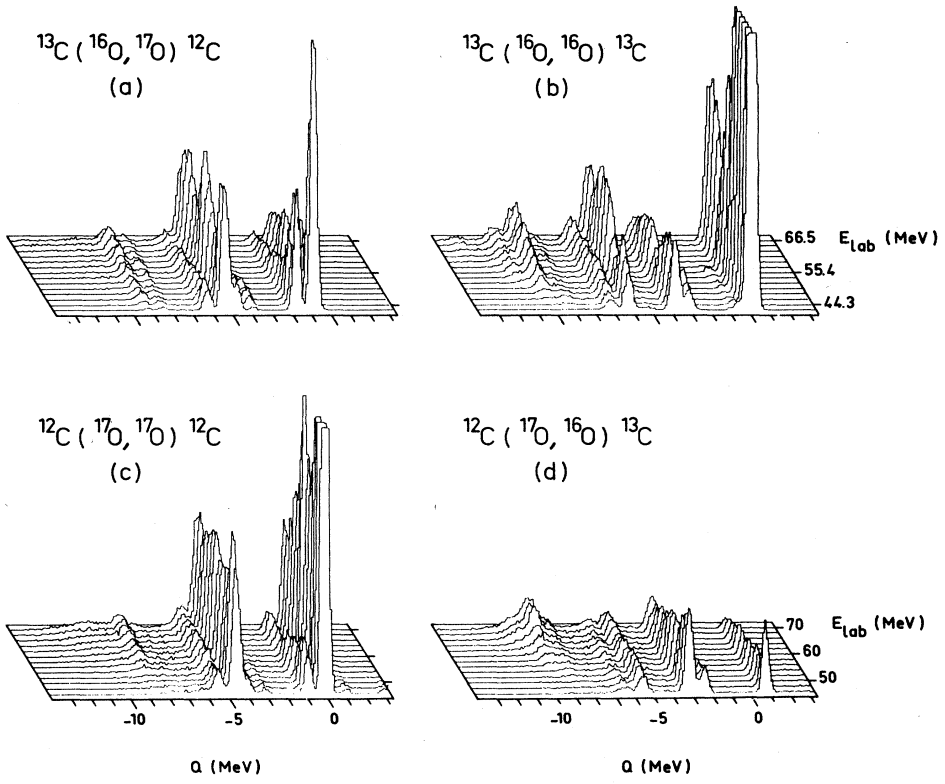

FIG. 1. Q-value spectra constructed from the coincident events for the four combinations with $^{13}C+^{16}O$ and $^{12}C+^{17}O$ as entrance and exit channels. They correspond to slices on our experimental data for an oxygen ejectile detected at laboratory angles between 25° and 28°. The vertical scales are identical and limited to 2000 counts.

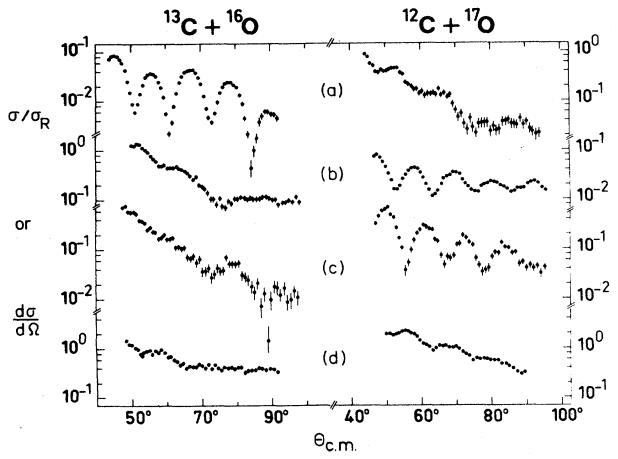

FIG. 2. Angular distributions of the $^{13}C+^{16}O$ reaction compared with $^{12}C+^{17}O$ at the same energy in the compound system for the following four outgoing channels: (a) $^{13}C_{g.s.}+^{16}O_{g.s.}$, (b) $^{12}C_{g.s.}+^{17}O_{g.s.}$, (c) $^{12}C_{g.s.}+^{17}O^*$ (0.871 MeV), (d) $^{12}C^*$ (4.44 MeV)$+^{17}O_{g.s.}$. The cross sections are divided by the Rutherford cross section for the elastic channels and in units of mb/sr for the reaction channels. The bombarding energies were 57.24 MeV for ^{16}O and 60 MeV for ^{17}O.

angular dependence. Though this was found to be true, it was observed that the angular distribution for the first excited state of ^{13}C ($E_x=3.09$ MeV, $J^\pi=\frac{1}{2}^+$) was highly structured. Here the situation may be similar to the inelastic excitation of the first excited state of ^{17}O where the valence neutron also occupies an $s_{1/2}$ orbital. Our results for the inelastic scattering to the first excited state of ^{17}O have been fitted by Voit and von Oertzen[5] with a distorted-wave Born approximation (DWBA) calculation.

The scattering angles were defined with respect to the oxygen ejectile. In the alternative case, where the ejectile is carbon, the angles were transformed from θ to $180°-\theta$, and correspond to large reaction angles. As a rule, intensities at the large angles were weak and these data were not thoroughly analyzed. However, three cases where we have extended our angular distribution out into this region are shown in Fig. 3.

III. EXPERIMENTAL RESULTS

A. Elastic scattering

Four typical elastic angular distributions for the $^{13}C+^{16}O$ reaction are shown in Fig. 4 compared with the $^{12}C+^{17}O$ data at the same center-of-mass energies. It is

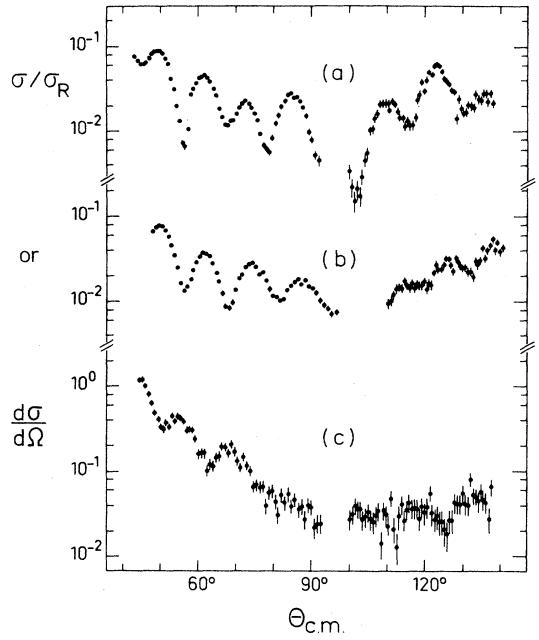

FIG. 3. Three examples where the angular distribution analysis was extended out to large angles: (a) $^{13}C+^{16}O$ elastic, (b) $^{12}C+^{17}O$ elastic, (c) $^{12}C+^{17}O \rightarrow {}^{13}C_{g.s.}+{}^{16}O_{g.s.}$. All distributions are for the same center-of-mass energy, i.e., $E_{c.m.}=22.3$ MeV. The cross sections are divided by the Rutherford cross section for the elastic channels and in units of mb/sr for the transfer channel.

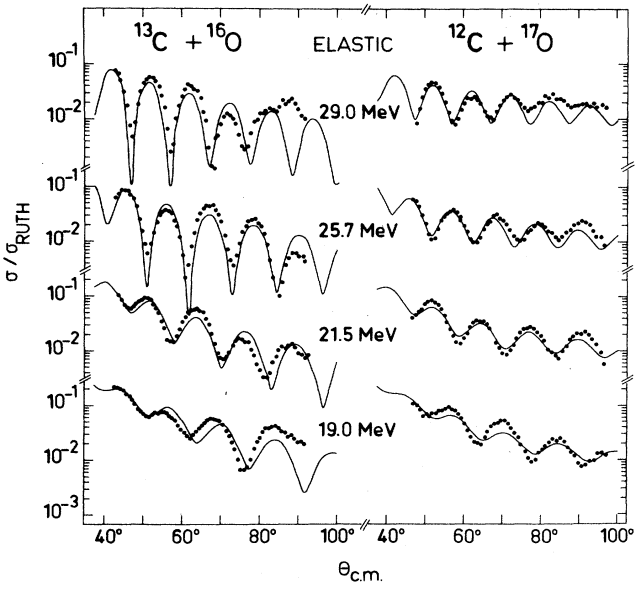

FIG. 4. Comparison between the $^{13}C+^{16}O$ and $^{12}C+^{17}O$ elastic angular distributions at four energies. The full lines are optical-model fits with parameters given in Table I. These fits reproduce the greater peak-to-valley ratios observed for the $^{13}C+^{16}O$ system.

immediately noticeable that, of the two entrance channels, the $^{13}C+^{16}O$ angular distributions are more highly structured. This characteristic also persists out to large scattering angles, as can be seen in Fig. 3, but we have only attempted to fit the forward-angle data where the reaction mechanism is more simple and the angular behavior more regular as a function of energy.

A six-parameter optical model was used to fit the forward-angle elastic scattering, as described in previous articles.[1,6] We have adopted a more general approach, however, in the present work with the intention of rendering the physical differences more explicit. Rather than fitting the angular distributions individually, we have searched for a set of parameters which are as common as possible to both systems. This parameter set is listed in Table I. It was found that the difference between the two systems could be adequately simulated by a greater diffusivity a_R in the real potential and a greater depth W in the imaginary potential for the $^{12}C+^{17}O$ system. The other parameters were identical for both systems.

The starting point for this parameter set was the potential Malmin[7] obtained to describe the $^{12}C+^{16}O$ elastic scattering. In fact, we have adopted his expression $7.5+0.4E_{c.m.}$ for the depth of the real potential. A smaller radius of the imaginary potential was required at higher energies, as also found by Pantis *et al.*[8] for the $^{16}O+^{16}O$ system. Other parameters were held constant with energy except for the depth of the imaginary potential, which was the only parameter allowed to vary freely in the final fitting.

The deeper imaginary potential in the case of the $^{12}C+^{17}O$ system is expected. It is the lesser bound of the two systems and it follows simply from Q-value considerations that more exit channels are open to contribute to the absorption. The greater diffusivity of the real potential could be attributed to the valence neutron. It is more weakly bound on ^{17}O than on ^{13}C and in a d rather than p orbital. An alternative point of view is that the Landau-Zener effect is more active in the $^{12}C+^{17}O$ reaction.[9] However, the influence of the Landau-Zener effect is still an open question[5,10] at these energies well above the Coulomb barrier, and quantitative comparison with theory is handicapped by the complexity of any real situation.

B. Excitation functions

The angular distributions displayed in Fig. 2 were integrated over a wide range of angles, and the resulting cross sections are displayed as a function of energy in Fig. 5. These integrations, calculated from the expression $2\pi \int d\sigma/d\Omega \sin\theta \, d\theta$, were performed over the forward angles with the exception of the elastic channel where potential scattering dominates at smaller angles. Apparent anomalies in the excitation functions can be generated as the diffraction pattern moved across the limited integration range. To minimize this effect we have used angular ranges, as specified in the caption of Fig.5, which embrace several cycles of the diffraction patterns. In the

TABLE I. Parameters for the optical-model fits to the $^{13}C+^{16}O$ and $^{12}C+^{17}O$ elastic data.

			a_R			W		
$E_{c.m.}$	r_{0R}	V	$^{13}C+^{16}O$	$^{12}C+^{17}O$	r_{0I}	$^{13}C+^{16}O$	$^{12}C+^{17}O$	a_I
19.0	1.35	15.1	0.51	0.58	1.40	5.0	9.2	0.30
21.5	1.35	16.1	0.51	0.58	1.39	6.7	12.1	0.30
25.7	1.35	17.8	0.51	0.58	1.38	6.7	17.1	0.30
29.0	1.35	19.1	0.51	0.58	1.37	9.1	22.7	0.30

upper two excitation functions, i.e., for the elastic and the $^{12}C^*(2^+)+^{17}O_{g.s.}$ channel, pronounced broad resonances are observed which are roughly correlated. A perusal of Fig. 1 suggests that similar structures occur in other channels, in particular the inelastic scattering of $^{13}C+^{16}O$ to states at about 4 and 6 MeV. The results displayed in this figure are restricted to a narrower angular window where changes in the angular distribution may conceivably be responsible for an apparent energy behavior. However, as mentioned in Sec. II, we have verified that the corresponding angular distributions are only weakly structured and should thus little influence the observed energy dependence. The states at 6 MeV are the (6.13-6.06) MeV levels of ^{16}O. Although this doublet cannot be resolved in the present experiments, it can be anticipated that it is the well-matched channel to the 3^- state ($E_x=6.13$ MeV) which is effectively responsible for the structure, rather than the other 0^+ member. The other peak corresponds to the (3.85-3.68) MeV doublet of ^{13}C. From matching arguments there is little preference for which state ($J^\pi=\frac{5}{2}^+$ and $\frac{3}{2}^-$) is most excited in this case.

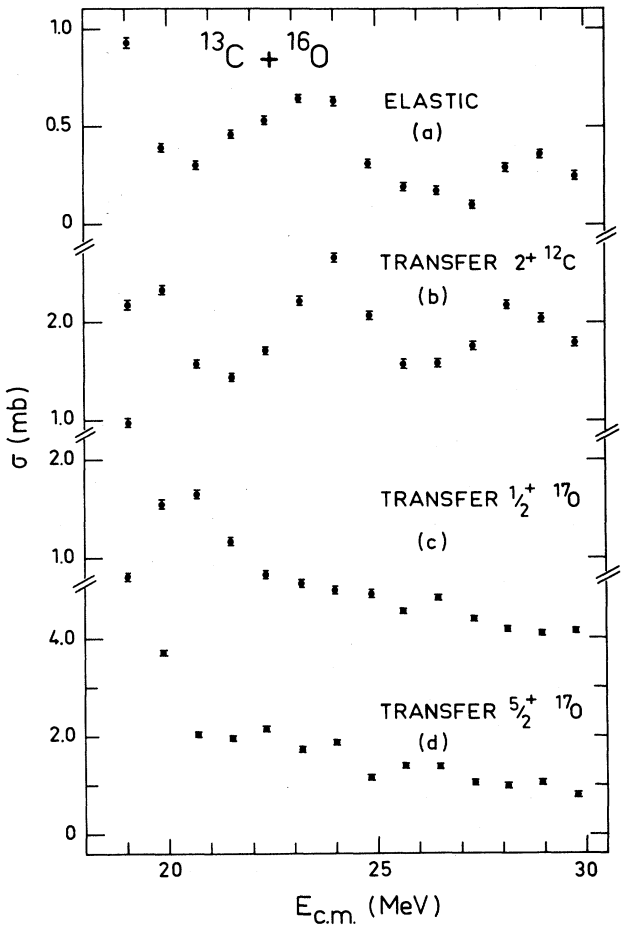

FIG. 5. Excitation functions of the $^{13}C+^{16}O$ reaction obtained by integration over the angular distributions. The results are displayed for the following four outgoing channels: (a) elastic (115°–135°), (b) $^{12}C^*$ (4.44 MeV)$+^{17}O_{g.s.}$ (55°–85°), (c) $^{12}C_{g.s.}+^{17}O^*$ (0.871 MeV) (50°–90°), (d) $^{12}C_{g.s.}+^{17}O_{g.s.}$ (50°–90°). The angles in parentheses indicate the range over which the integration was performed.

This type of gross structure is frequently encountered in such heavy-ion reactions. It is generally admitted that they arise from shape resonances in the entrance channel which are coupled to similar resonances in the exit channels. They appear in channels where the coupling is strong, for example, where collective states, like the 2^+ state of ^{12}C or the 3^- state of ^{16}O, are excited. The successive maxima are separated by energies which are roughly equivalent to a change of two units of l_g, the grazing angular momentum, suggesting that parity dependence plays an important part in enhancing the shape resonances. Tanimura[11] included a parity-dependent part in the potential he used to generate shape resonances for this reason. The fact that this type of structure appears more prominently in $^{13}C+^{16}O$ than in $^{12}C+^{17}O$ reactions is probably just a question of transparency. In the more strongly absorbing $^{12}C+^{17}O$ system, the shape resonances are more strongly attenuated.

We have also measured[12] γ-ray yields from the $^{13}C+^{16}O$ and $^{12}C+^{17}O$ reactions. These measurements were performed mainly at lower energies, but they overlapped to some extent with our energy domain. Structures like those of Fig. 5 were barely discernable in these γ-ray yield functions, but a detailed comparison between the results of the two methods is not possible. The γ-ray intensities are the sum of all channels leading to the same γ-ray emitting state. It is therefore not surprising that the structures stand out more clearly in our measurements where the channels are selected in a more exclusive manner. On the other hand, the particle angular distributions are much more complex and, unless measurements are made over the whole domain, angular effects are not entirely eliminated from the excitation functions.

A different type of energy dependence is observed for the other two channels shown in the lower half of Fig. 5. The structure here is relatively minor and may disappear totally if the integration could be carried out over a com-

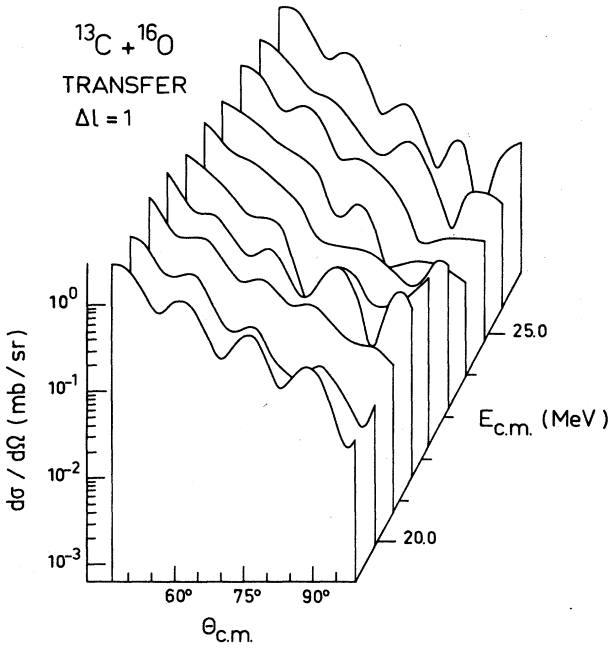

FIG. 6. Angular distributions measured for the $^{13}C+^{16}O\rightarrow{}^{12}C_{g.s.}+^{17}O^*$ (0.871 MeV) reaction. In its simplest form the reaction mechanism can be considered as a $\Delta l_n=1$ transfer of the valence neutron from a $p_{1/2}$ to $s_{1/2}$ orbit. The rapid variation of the distributions with energy illustrates that the effective mechanism is more complex.

plete 4π geometry. The excitation function in Fig. 5(d) has previously been measured[1] for the inverse reaction $^{12}C+^{17}O\rightarrow{}^{13}C+^{16}O$ for the same angular conditions. The same structures, though shifted of course by the 0.8 MeV difference in binding energy, are confirmed by the present results.

These two channels correspond to the transfer of a neutron from single-particle states on a ^{12}C to an ^{16}O core. The mechanism is complicated by the possibility that the neutron can occupy molecular orbits during the process and the resulting interference will lead to erratic behavior of the energy dependence. This interference is probably the origin of the minor structure observed in the excitation functions of Figs. 5(c) and (d). Signatures of this interference should show up clearly in the angular distributions, particularly for $\Delta l=1$ transfers which are known to be the most sensitive to details in the reaction dynamics.[13] A case in point is the channel shown in Fig. 5(c), where the neutron is transferred from a $p_{1/2}$ orbit in ^{13}C to the $s_{1/2}$ orbital of the first excited state of ^{17}O. The excitation function for this channel contains only a little structure, but the changes in angular distribution in the same energy range, as shown in Fig. 6, are remarkable. The rapid fluctuations in form with energy testify to the complexity of the reaction mechanism and constitute indirect evidence for the role of molecular orbital formation during the collision process.

IV. CONCLUSIONS

We have studied the $^{13}C+^{16}O$ reaction by the same method and over the same energy range as our previous work on $^{12}C+^{17}O$. Two features of this work indicate a greater transparency of the $^{13}C+^{16}O$ system; firstly, more highly structured elastic angular distributions and secondly, shape resonances are more evident in the outgoing channels. Both collective and single-particle variables play important roles in the reaction mechanisms. Collective states like the 2^+, first excited state of ^{12}C and the 3^- second excited state of ^{16}O are relatively strongly excited and resonate with the entrance channel. Channels which involve a rearrangement of the single-particle states have cross sections and angular distributions which show a more complex and erratic behavior with energy. This is interpreted as a consequence of the interference with molecular orbital formation during the nuclear collision.

[1]R. M. Freeman, C. Beck, F. Haas, A. Morsad, and N. Cindro, Phys. Rev. C **33**, 1275 (1986).
[2]N. Cindro, R. M. Freeman, and F. Haas, Phys. Rev. C **33**, 1280 (1986).
[3]G. A. Westfall and S. A. A. Zaidi, Phys. Rev. C **14**, 610 (1976).
[4]R. L. Parks, S. T. Thornton, K. R. Cordell, and C.-A. Wiedner, Phys. Rev. C **25**, 313 (1982).
[5]H. Voit and W. von Oertzen, Phys. Rev. C **35**, 2321 (1987).
[6]S. Datta, N. Cindro, R. M. Freeman, C. Beck, F. Haas, and A. Morsad, Fizica **19**, 445 (1987).
[7]R. E. Malmin, Ph.D. thesis, Argonne National Laboratory, 1972.
[8]G. Pantis, K. Ioannidis, and P. Poirier, Phys. Rev. C **32**, 657 (1985).
[9]A. Thiel, W. Greiner, and W. Scheid, J. Phys. G **14**, L85 (1988).
[10]B. Milek and R. Reif, Phys. Lett. **157B**, 134 (1985).
[11]O. Tanimura, Z. Phys. A **319**, 227 (1984).
[12]C. Beck, R. M. Freeman, F. Haas, B. Heusch, and J. J. Kolata, Nucl. Phys. **A443**, 157 (1985).
[13]B. Imanishi and W. von Oertzen, Phys. Rep. **155**, 29 (1987).